Poroelastic swelling kinetics of thin hydrogel layers: comparison of theory and experiment

Jinhwan Yoon,[a] Shengqiang Cai,[b] Zhigang Suo*[b] and Ryan C. Hayward*[a]

Thin poly(N-isopropylacrylamide) (PNIPAM) hydrogels were allowed to swell under two conditions: as freestanding layers and as substrate-attached layers. Through a combination of particle tracking and defocusing methods, the positions of beads embedded within the gels were monitored over time *via* fluorescence microscopy, providing a convenient method to track the kinetics of swelling for layers with thicknesses of the order 100 μm. These data are compared with the predictions of linear poroelastic theory, as specialized for polymer gels. This theory, along with a single set of material properties, accurately describes the observed swelling kinetics for both the freestanding and substrate-attached hydrogels. With the additional measurement of the substrate curvature induced by the swelling of the substrate-attached hydrogels, these experiments provide a simple route to completely characterize the material properties of the gel within the framework of linear poroelasticity, using only an optical microscope.

Introduction

A network of covalently crosslinked polymers may imbibe a larger quantity of a solvent, resulting in a polymer gel. The gel behaves as an elastic solid due to the presence of the polymer network, yet can transport matter due to the mobility of the solvent. These combined solid and liquid attributes lead to unique properties that make gels ubiquitous in nature and engineering. Gels constitute many biological tissues and are used in diverse applications, such as carriers for drug delivery,[1,2] actuators and sensors,[3,4] tissue engineering matrices,[5,6] and packers in oilfields.[7,8]

In a polymer gel, deformation of the network and transport of the solvent are concurrent processes. While polymer gels are capable of large deformations that require a non-linear theory to analyze fully,[9–13] linear theories have met with remarkable success in describing even moderately large deformations. One such linear theory for polymer gels is due to Tanaka and co-workers.[14,15] Owing to the assumption of negligible fluid displacements, this theory fails to capture some of the most salient experimental observations.[16–18] It has been appreciated that concurrent deformation and transport in gels can be described using Biot's theory of linear poroelasticity, which does not suffer from the same limitations.[19–25] Meanwhile the theory of Tanaka and co-workers, despite its inadequacies, remains the dominant theory in the literature to describe swelling kinetics of polymer gels.[26–34] This situation stems at least partially from the fact that relatively little work has been done to compare the predictions of linear poroelastic theory to experiments on swelling kinetics.[20]

In the current article, we seek to fulfill three objectives. First, we reproduce the derivation of Biot's theory explicitly in terms of polymer gels, yielding a set of differential equations that represent a straightforward route to model swelling kinetics for gels with arbitrary geometries and boundary conditions. Second, we show that the theory, along with a single set of material parameters, accurately describes the experimentally measured swelling kinetics of a poly(N-isopropylacrylamide) (PNIPAM) hydrogel under the two conditions shown in Fig. 1, namely, a thin gel layer undergoing swelling either freely in 3D (subject to no external constraints) or only in 1D due to the constraint imposed by attachment to a rigid substrate. Both of these cases have previously been analyzed separately in terms of Tanaka's theory,[26–34] though we are unaware of any cases where they have been considered side-by-side on the same material system to provide a more stringent validation of the theory. Finally, we show that these two experiments, combined with a measurement of the substrate curvature induced in the case of 1D swelling, provide a straightforward route to completely characterize the material properties of the gel within the framework of linear poroelasticity, yielding the modulus, Poisson's ratio, and permeability of the gel. Thus, in addition to establishing the
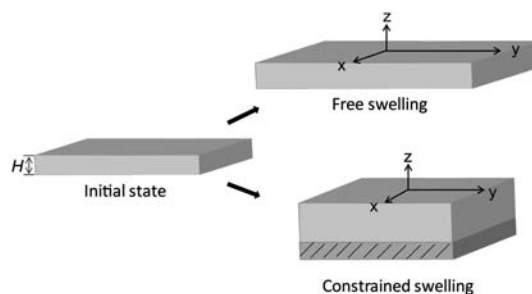
[a]Department of Polymer Science & Engineering, University of Massachusetts, Amherst, MA, 01003, USA. E-mail: rhayward@mail.pse.umass.edu; Tel: +1 413-577-1317
[b]School of Engineering and Applied Sciences, Kavli Institute, Harvard University, Cambridge, MA, 02138, USA. E-mail: suo@seas.harvard.edu; Tel: +1 617-495-3789

Fig. 1 A schematic illustrating the two geometries considered experimentally and theoretically here: free three-dimensional swelling and constrained one-dimensional swelling of thin gel layers ($H = 76$–504 μm).

adequacy of linear poroelasticity to describe swelling kinetics of polymer gels, we anticipate that our approach will provide a useful tool to characterize the properties of gel films using no equipment other than an optical microscope.

Materials and methods

Preparation of freestanding and substrate-attached hydrogels

Thin layers of poly(N-isopropylacrylamide) hydrogels were prepared by mixing 200 µL of a degassed aqueous pre-gel solution containing 878 mM N-isopropylacrylamide and 4.4 mM N,N′-methylenebis(acrylamide) with 0.3 µL of N,N,N′,N′-tetramethylethylenediamine, 1.0 µL of a 10 wt% aqueous ammonium persulfate solution, and a small amount (0.2–2.0 µL) of a diluted suspension of fluorescent polystyrene beads (diameter 1 or 3 µm, Polysciences) in water. The concentration of the bead solution and the volume added to the pre-gel mixture were chosen to yield an average of ∼10 to 20 beads in an area of ∼1 mm². The mixture was loaded by capillary action between a substrate and a bare coverslip separated by spacers (Kapton HN films, DuPont, or glass coverslips) to define the thickness of the gel, which was varied from 76 to 504 µm. Gelation, carried out in a sealed chamber under positive pressure of nitrogen, was allowed to proceed for 30 min before separating the bare coverslip from the gel. To anchor gels to substrates and restrict their swelling to 1D, coverslip substrates were treated with the adhesion-promoter [3-(methacryloxy)propyl] trimethoxysilane, such that the gel formed covalent attachments to the substrate during polymerization. To prepare freestanding gels capable of swelling in 3D, a bare coverslip was instead used as a substrate, allowing the gel to be readily detached from the substrate.

Measurement of swelling kinetics

Following gelation, gels were immersed in deionized water and swelling kinetics were monitored using epi-fluorescence microscopy (Zeiss Axiovert 200, 10× objective). For surface-attached gels, the apparent sizes of the fluorescent beads were measured as a function of time. At a fixed vertical position of the microscope stage and objective, changes in the vertical positions of beads due to swelling of the hydrogel changed the defocusing of each bead and thus its size in the resulting image.[35,36] The vertical position of the bead was determined from a calibration curve of defocusing induced by a translation of the microscope objective by a known distance. We verified that the same translation of beads in an aqueous environment (at fixed objective position) yielded equivalent changes in the sizes of the defocused images, thus no corrections were necessary to account for refractive index mismatches.[37] For each gel, at least 5 beads within 40 µm of the free surface were tracked to provide the time-dependent swelling of the gel, characterized by the total thickness of the substrate-attached gel divided by its initial thickness, with error bars reflecting the standard deviation.

For the freestanding gels, the in-plane swelling was monitored instead of the vertical swelling, since this provided smaller uncertainties in the reported values. As described below, the lateral swelling of the gel at any point in time is equal to the vertical swelling. To measure lateral swelling, the positions of a collection of at least 10 fluorescent beads were tracked as a function of time. At each time point, the distance of each bead from the center of mass of the collection divided by its initial distance yielded the in-plane swelling. Values determined for each bead were averaged, with uncertainties taken as the standard deviation.

Measurement of swelling stress

To measure the change in substrate curvature induced by swelling stresses, 504 µm thick PNIPAM gel layers of lateral dimensions 37 mm by 5.7 mm and 31 mm by 5.6 mm were prepared on 76 and 126 µm thick Kapton substrates, respectively. Kapton substrates, with Young's modulus of 2.5 GPa and Poisson's ratio of 0.34 as reported by the manufacturer, were degassed for 12 h prior to gelation to remove oxygen that otherwise interferes with free radical polymerization and alters the material properties of the gel. The Kapton substrates were also treated with the adhesion-promoter [3-(methacryloxy)-propyl]trimethoxysilane to improve adhesion of the gel to the substrate. A bare Kapton substrate was also found to undergo a small change in curvature (0.08 m⁻¹) when immersed in water; this amount has been included in the stated uncertainties for the measured curvatures of the supported gel samples.

Shear rheology

Independent measurements of the shear modulus of PNIPAM gels were performed using a rheometer (AR 2000ex, TA Instruments) equipped with a 40 mm diameter aluminium parallel plate and solvent trap to avoid evaporation. Shear moduli were estimated from the values of storage modulus (G') in the plateau region from frequency sweeps over the range of 100 rad s⁻¹ to 0.01 rad s⁻¹ at a constant stress of 1 Pa. Gels were measured in the unswelled state (just after polymerization), as well as following unconstrained 3D swelling to equilibrium in water.

Background and analysis

An outline of Biot's theory of poroelasticity

To set up notation, we outline Biot's theory of poroelasticity. The theory was originally developed to analyze migration of liquids in soils,[22] and has been adapted in recent years to analyze migration of solvent in polymer networks.[20–25] The initial state of the gel is taken to be homogenous, subject to no mechanical load, with C_0 being the concentration of the solvent in the gel (i.e., the number of solvent molecules per unit volume of the gel) and μ_0 being the chemical potential of the solvent in the gel. When the gel deforms from the initial state, the displacement is a time-dependent field, $u_i(x_1,x_2,x_3,t)$, giving rise to a field of strain:

$$\varepsilon_{ij} = \frac{1}{2}\left(\frac{\partial u_i}{\partial x_j} + \frac{\partial u_j}{\partial x_i}\right). \tag{1}$$

The concentration of the solvent in the gel is also a time-dependent field, $C(x_1,x_2,x_3,t)$. The number of solvent molecules is conserved, so that

$$\frac{\partial C}{\partial t} + \frac{\partial J_k}{\partial x_k} = 0, \tag{2}$$

where J_k is the flux of the solvent.

The gel is in mechanical equilibrium, so that the field of stress $\sigma_{ij}(x_1,x_2,x_3,t)$ satisfies

$$\partial\sigma_{ij}/\partial x_j = 0 \tag{3}$$

The gel, however, is not in diffusive equilibrium, so that the chemical potential of the solvent in the gel is a time-dependent field, $\mu(x_1,x_2,x_3,t)$. The migration of the solvent in the gel is taken to obey Darcy's law:

$$J_i = -\left(\frac{k}{\eta\Omega^2}\right)\frac{\partial\mu}{\partial x_i} \tag{4}$$

where k is the permeability of the gel, η the viscosity of the solvent, and Ω the volume per solvent molecule. The values of η and Ω are generally well known for a given solvent, so that eqn (4) defines the permeability of the gel k, which has the dimensions of length squared.

Each element of the gel is assumed to be in local thermodynamic equilibrium, so that the work done to the element equals the change in the free energy:

$$\delta W = \sigma_{ij}\delta\varepsilon_{ij} + (\mu - \mu_0)\delta C, \tag{5}$$

where W is the Helmholtz free energy per unit volume of the gel, $\sigma_{ij}\delta\varepsilon_{ij}$ the work done by the stress, and $(\mu - \mu_0)\delta C$ the work done by the chemical potential. The network polymers and the solvent molecules are commonly assumed to be incompressible.[20–25] Consequently, the increase in the volume of the gel is entirely due to the additional solvent molecules absorbed, namely,

$$\varepsilon_{kk} = \Omega(C - C_0). \tag{6}$$

The concentration of the solvent is no longer an independent variable, and the free energy is a function $W(\varepsilon_{11}, \varepsilon_{12}, \ldots)$, with the six components of the strain being independent variables. Inserting eqn (6) into eqn (5), we obtain

$$\sigma_{ij} = \frac{\partial W(\varepsilon_{11}, \varepsilon_{12}, \ldots)}{\partial\varepsilon_{ij}} - \frac{\mu - \mu_0}{\Omega}\delta_{ij}, \tag{7}$$

where $\delta_{ij} = 1$ when $i = j$ and $\delta_{ij} = 0$ when $i \neq j$. In a linear theory of an isotropic gel, the free energy is taken to be quadratic in the strain:

$$W = G\left[\varepsilon_{ij}\varepsilon_{ij} + \frac{\nu}{1 - 2\nu}(\varepsilon_{kk})^2\right]. \tag{8}$$

where G is the shear modulus and ν is Poisson's ratio.

A combination of eqn (7) and (8) gives

$$\sigma_{ij} = 2G\left(\varepsilon_{ij} + \frac{\nu}{1 - 2\nu}\varepsilon_{kk}\delta_{ij}\right) - \frac{\mu - \mu_0}{\Omega}\delta_{ij}. \tag{9}$$

The quantity $(\mu - \mu_0)/\Omega$ is known as the pore pressure in the theory of poroelasticity and as the water potential in plant physiology. To appreciate the significance of the two constants G and ν, consider a hypothetical experiment with a rod of a gel immersed in an external solvent of chemical potential μ_0 (Fig. 2). Initially the rod is in equilibrium with the external solvent, with μ_0 being the chemical potential of solvent in the gel, and C_0 the concentration of solvent in the gel. The rod is suddenly pulled to a fixed strain ε_{zz}. Right after pulling, the solvent has no time to migrate, so that $C = C_0$ and $\varepsilon_{kk} = 0$, and the gel behaves like an
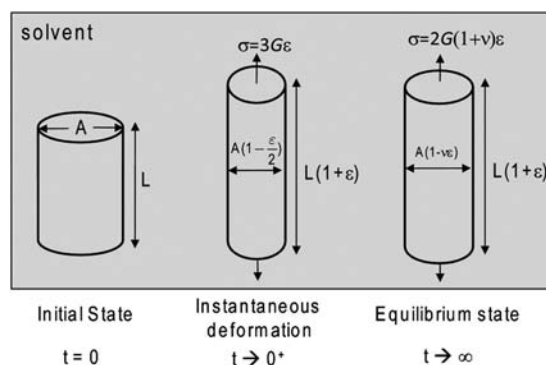

Fig. 2 A hypothetical experiment involving uniaxial stretching of a cylinder of gel immersed in solvent. Immediately following deformation, the material acts as an incompressible elastic solid with Poisson's ratio ½, however, over time the chemical potential of solvent in the gel equilibrates with the surroundings, leading to expansion in the lateral dimension and an apparent Poisson's ratio ν.

incompressible elastic solid of shear modulus G, giving $\varepsilon_{xx} = \varepsilon_{yy} = -\varepsilon_{zz}/2$, $(\mu - \mu_0)/\Omega = -G\varepsilon_{zz}$, $\sigma_{xx} = \sigma_{yy} = 0$ and $\sigma_{zz} = 3G\varepsilon_{zz}$. Pulling causes the chemical potential of solvent in the gel, μ, to drop below the chemical potential of the solvent outside the gel, μ_0. Consequently, the gel imbibes more solvent over time, the volume of the gel increases, and the pulling force on the gel relaxes. After a long time, the solvent in the gel equilibrates with the external solvent, $\mu = \mu_0$, so that the gel behaves like a compressible elastic solid of shear modulus G and Poisson's ratio ν, giving $\varepsilon_{xx} = \varepsilon_{yy} = -\nu\varepsilon_{zz}$, $\sigma_{xx} = \sigma_{yy} = 0$ and $\sigma_{zz} = 2(1 + \nu)G\varepsilon_{zz}$. In this new state of equilibrium, the volumetric strain is $\varepsilon_{kk} = (1 - 2\nu)\varepsilon_{zz}$. Thus, Poisson's ratio indicates the ability of a gel to imbibe additional solvent in response to the pulling.

Eqn (1)–(4), (5) and (9) specify the governing equations for the time-dependent fields u_i, ε_{ij}, C, μ, J_i, and σ_{ij}. This set of equations can be reduced to equations governing the fields u_i and μ, namely,

$$G\left(\frac{\partial^2 u_i}{\partial x_k\partial x_k} + \frac{1}{1 - 2\nu}\frac{\partial^2 u_k}{\partial x_k\partial x_i}\right) = \frac{\partial\mu}{\partial x_i}, \tag{10}$$

$$\frac{\partial C}{\partial t} = D\frac{\partial^2 C}{\partial x_k\partial x_k}, \tag{11}$$

with the concentration of solvent related to the divergence of the displacement, $\partial u_k/\partial x_k = \Omega(C - C_0)$, and the diffusivity given by

$$D = \frac{2(1 - \nu)Gk}{(1 - 2\nu)\eta}. \tag{12}$$

Eqn (10) expresses the condition of mechanical equilibrium, where the gradient of the chemical potential serves the role of a body force. Eqn (11) takes the familiar form of the diffusion equation. In poroelasticity, however, this diffusion equation cannot be solved by itself, because the boundary conditions typically involve the chemical potential and the displacement. Nonetheless, eqn (11) indicates that over time t a disturbance diffuses over a length $\sqrt{Dt}$.

Swelling of a thin gel layer attached to a substrate

We now examine the case of constrained (1D) swelling, as illustrated in Fig. 1. This problem has been studied before,[20] and a similar problem was examined in Biot's 1941 paper.[19] Here we discuss the aspects of solution that can be directly compared with our experiments. Right after gelation, the gel is taken to be in a homogeneous state, with C_0 being the concentration of the solvent in the gel and μ_0 the chemical potential. The gel is then immersed in an external solvent of chemical potential $\bar{\mu}$. The excess in the chemical potential, $\bar{\mu} - \mu_0$, drives the solvent to migrate into the gel. The in-plane dimensions of the gel are much larger than its thickness, so that the gel absorbs solvent mostly from its top surface, and negligibly from its edges. As such, the flux is entirely in the thickness direction and is a function of position and time. The displacement in the thickness direction, $u_z(z,t)$, and the chemical potential of solvent, $\mu(z,t)$, are also functions of time and position. As the solvent migrates into the network, the in-plane dimensions of the gel remains unchanged, $\varepsilon_{xx} = \varepsilon_{yy} = 0$, but in-plane stresses $\sigma_{xx}(z,t) = \sigma_{yy}(z,t)$ are generated. The gel is subject to no force from the top, so $\sigma_z = 0$. Inserting these conditions into eqn (9), we obtain

$$\frac{\partial u_z}{\partial z} = \frac{(1-2\nu)(\mu - \mu_0)}{2(1-\nu)G\Omega}, \tag{13}$$

$$\sigma_{xx} = \frac{\mu - \mu_0}{(1-\nu)\Omega}. \tag{14}$$

The resultant force per unit length is defined by $f(t) = \int_{-H}^{0} \sigma_{xx}(z,t)\,\mathrm{d}z$. A combination of eqn (13) and (14) gives

$$\Delta(t) = \frac{1-2\nu}{2G} f(t), \tag{15}$$

where $\Delta(t) = u_z(0,t)$ is the change in the thickness of the layer. Thus, once an expression for $\Delta(t)$ is obtained, eqn (15) gives a similar expression for $f(t)$.

Darcy's law eqn (4) becomes

$$\frac{\partial \mu}{\partial t} = D \frac{\partial^2 \mu}{\partial z^2}. \tag{16}$$

The initial condition is $\mu(z,0) = \mu_0$, while the boundary conditions are $\mu(0,t) = \bar{\mu}$ at the top surface and $\partial\mu/\partial z = 0$ as the bottom surface ($z = -H$). These conditions, along with eqn (16), govern the function $\mu(z,t)$. This problem takes the same form as the diffusion problem treated in many textbooks.

The thickness of the layer, H, is much smaller than the lateral dimensions, so that the solvent needs to migrate over the thickness of the gel to equilibrate its chemical potential. After a long time, $\sqrt{Dt} \gg H$, the gel equilibrates, *i.e.*, the chemical potential of solvent in the gel, μ, becomes homogeneous and equal to $\bar{\mu}$. Thus, inserting $\mu = \bar{\mu}$ into eqn (13), we obtain the equilibrium change in thickness of the gel:

$$\Delta(\infty) = \frac{(1-2\nu)(\bar{\mu} - \mu_0)H}{2(1-\nu)G\Omega}. \tag{17}$$

At short times, $\sqrt{Dt} \ll H$, the chemical potential evolves by a self-similar profile:

$$\frac{\mu(z,t) - \bar{\mu}}{\mu_0 - \bar{\mu}} = erfc\left(-\frac{z}{2\sqrt{Dt}}\right). \tag{18}$$

Inserting eqn (18) into eqn (13) and integrating, we obtain the change in the thickness of the gel

$$\frac{\Delta(t)}{\Delta(\infty)} = \frac{2}{H}\sqrt{\frac{Dt}{\pi}}. \tag{19}$$

The complete transient solution is obtained by the separation of variables, giving

$$\frac{\mu(z,t) - \bar{\mu}}{\mu_0 - \bar{\mu}} = -\frac{4}{\pi}\sum_{n=0}^{\infty}\frac{1}{2n+1}\sin\left[\frac{(2n+1)\pi z}{2H}\right]\exp\left[-\frac{(2n+1)^2 t}{\tau}\right] \tag{20}$$

with

$$\tau = \frac{4H^2}{\pi^2 D}. \tag{21}$$

Inserting eqn (20) into eqn (13) and integrating, we obtain the displacement:

$$\frac{u_z(z,t)}{\Delta(\infty)} =$$
$$1 - \frac{8}{\pi^2}\sum_{n=0}^{\infty}\frac{1}{(2n+1)^2}\cos\left[\frac{(2n+1)\pi z}{2H}\right]\exp\left[-\frac{(2n+1)^2 t}{\tau}\right] + \frac{z}{H}. \tag{22}$$

The change of the thickness is

$$\frac{\Delta(t)}{\Delta(\infty)} = 1 - \frac{8}{\pi^2}\sum_{n=0}^{\infty}\frac{1}{(2n+1)^2}\exp\left[-\frac{(2n+1)^2 t}{\tau}\right]. \tag{23}$$

We note that an equivalent expression was derived by Doi[20] and by Peters and Candau.[26,27]

Swelling of a thin layer subject to no external constraints

We next consider unconstrained swelling; as before, immediately after gelation the concentration and chemical potential of solvent in the gel are C_0 and μ_0, respectively. Now, however, when subsequently immersed in an external solvent of chemical potential $\bar{\mu}$, the gel is free to expand in all three dimensions. After a long time, the gel equilibrates with the external solvent, so that the chemical potential of the solvent in the gel equals that in the external solvent, $\mu = \bar{\mu}$. Because the gel is freestanding, all components of the stress vanish at equilibrium. Inserting $\mu = \bar{\mu}$ and $\sigma_{ij} = 0$ into eqn (9), we obtain the three components of strain at equilibrium,

$$\varepsilon_{xx} = \varepsilon_{yy} = \varepsilon_{zz} = \frac{(1-2\nu)(\bar{\mu} - \mu_0)}{2(1+\nu)G\Omega}. \tag{24}$$

The change of the thickness of the layer at equilibrium is

$$\Delta(\infty) = \frac{(1-2\nu)(\bar{\mu} - \mu_0)H}{2(1+\nu)G\Omega}. \tag{25}$$

We next consider the transient solution. The chemical potential of the solvent in the gel is a time-dependent field, $\mu(z,t)$, with the initial condition $\mu(z,0) = \mu_0$ and the boundary conditions

$\mu(0,t) = \mu(-H,t) = \bar{\mu}$. Here we have assumed the condition of local equilibrium: when the gel is immersed in the external solvent and the chemical potential of the solvent at the surfaces of the gel instantaneously reaches that of the external solvent. The vertical displacement is also a time-dependent field, $u_z(z,t)$, with the initial condition $u_z(z,0) = 0$ and the boundary condition $u(-H,t) = 0$. Here we have fixed the position of the bottom surface to remove the rigid body motion. Unlike the gel attached to the substrate, the freestanding gel can swell in all three directions. Because the thickness of the gel is small compared to the lateral dimensions of the gel, the in-plane strains are time-dependent, but are independent of the depth, $\varepsilon_{xx}(t) = \varepsilon_{yy}(t)$.

We next list the equations that govern $\mu(z,t)$, $u_z(z,t)$ and $\varepsilon_{xx}(t)$. Substituting the condition of mechanical equilibrium, $\sigma_z = 0$, into eqn (9), we obtain

$$2G\left(\frac{1-\nu}{1-2\nu}\right)\frac{\partial u_z}{\partial z} + 4G\left(\frac{\nu}{1-2\nu}\right)\varepsilon_{xx} = \frac{\mu - \mu_0}{\Omega}, \qquad (26)$$

The condition of mechanical equilibrium in direction x is specified by the vanishing resultant force:

$$\int_{-H}^{0} \sigma_{xx}\,\mathrm{d}z = 0. \qquad (27)$$

A combination of eqn (9), (26) and (27) gives

$$\varepsilon_{xx}(t) = \frac{u_z(0,t)}{H}. \qquad (28)$$

This equation means that the in-plane swelling is equivalent to the average vertical swelling at all times, and thus the shape of the layer does not change during swelling.[18] The kinetic equation for the free-swelling layer becomes

$$\frac{\partial \mu}{\partial t} + 4G\Omega\frac{\mathrm{d}\varepsilon_{xx}}{\mathrm{d}t} = D\frac{\partial^2 \mu}{\partial z^2}. \qquad (29)$$

Unlike the constrained film, there is no self-similar solution for the freestanding layer in the initial stages. Since the in-plane strain is always equal to the average strain in thickness direction, in-plane deformation cannot be neglected even at short times. Eqn (26), (28) and (29) are coupled. Despite all of the modifications that have been made to Tanaka and co-workers' theory to treat different geometries,[19-25] apparently no one has numerically solved this partial differential equation to model swelling of a freestanding polymer gel layer. We will discuss our numerical solutions in conjunction with experimental data.

Results and discussion

To measure the swelling kinetics of thin gel layers we used a combination of fluorescent microparticle tracking and defocusing methods, as exemplified by the fluorescence images in Fig. 3. By measuring the defocusing of beads in constrained gels, the vertical displacement of the gel's free surface could be determined with a typical uncertainty of ±6%, even for gels as thin as 76 μm. In this case, we report the change in thickness of the gel normalized by its initial thickness, $\Delta(t)/H$. For 3D swelling of unconstrained gels, we instead determined the in-plane dilation $\varepsilon_{xx}(t)$ which could be measured with smaller
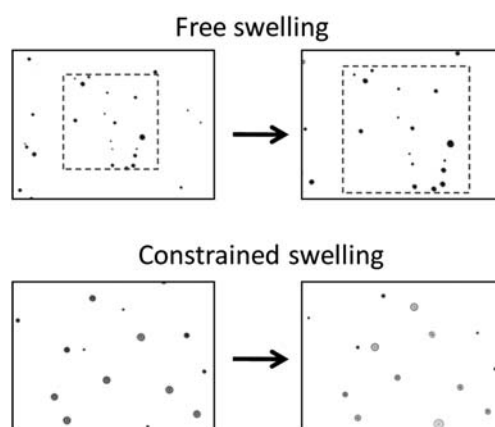

Fig. 3 Representative fluorescence micrographs of beads used to track swelling of constrained and unconstrained gels. For free swelling of unconstrained gels, the in-plane dilation of distances between a collection fluorescent beads, for example those within the dashed square, were tracked as a function of time. For constrained swelling of surface-attached gels, the apparent sizes of the fluorescent beads were measured as a function of time, revealing their distance from the focal plane of the microscope. The dimensions of each image are 1.6×1.2 mm.
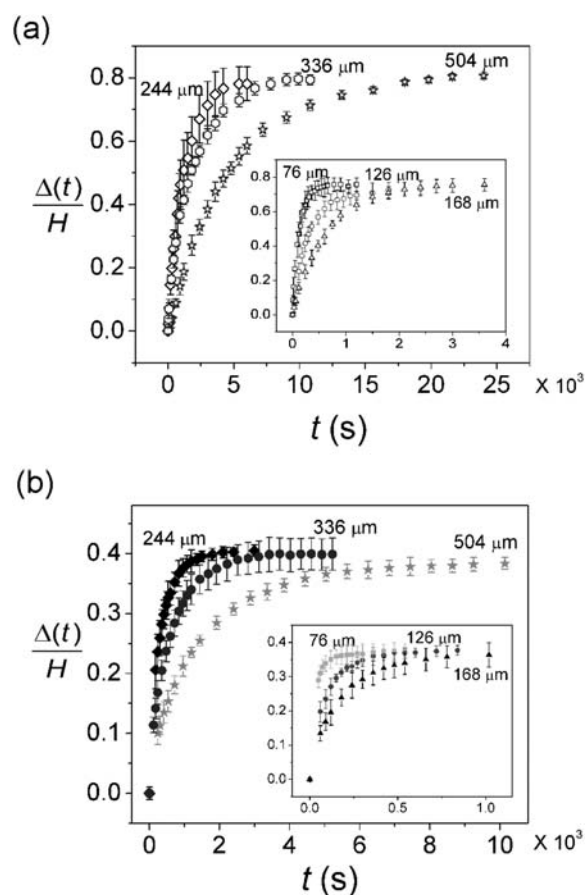

Fig. 4 Swelling curves for (a) constrained and (b) freestanding poly-(N-isopropylacrylamide) hydrogel films with different initial thicknesses ($H = 76$–504 μm) after immersion in deionized water at $t = 0$. Values were determined by tracking the vertical displacements of fluorescent beads in (a) and the lateral displacement of fluorescent beads in (b).

uncertainty (±3%), and according to eqn (28) is identical to $\Delta(t)/H$. While this equivalence has been experimentally demonstrated by Tanaka and co-workers,[16] we confirmed this point for the PNIPAM gels considered here by comparing the lateral and vertical swelling of a freestanding film with $H = 504$ µm as a function of time (data not shown), which were found to be the same within experimental uncertainty.

Results for 1D and 3D swelling kinetics of PNIPAM gel layers of varying thickness are presented in Fig. 4. The most striking difference between swelling in 1D vs. 3D is the substantially larger equilibrium change in linear dimension of the constrained gel. Indeed, a comparison between eqn (17) and (25) reveals that the value of $\Delta(\infty)$ for the constrained gel should be larger than that for the unconstrained gel by a factor of $(1 + \nu)/(1 - \nu)$, which is notable since it is determined by Poisson's ratio alone. The experimental data in Fig. 4 yield a value for this ratio of 2.0, indicating the Poisson's ratio of the gel is $\nu = 0.33$. We note that this method of determining Poisson's ratio was described previously by Li et al.,[38] who reported ν in the range of 0.25–0.36 for polyacrylamide gels containing 5 wt% monomer. Somewhat lower values (0.13–0.20) were determined by Oyen and co-workers[24] for more concentrated acrylamide gels (20 wt% monomer), while two studies on PNIPAM gels yielded Poisson's ratios of 0.25–0.4 in the swelled state.[39,40] Thus, the value determined here is in reasonable agreement with prior reports for similar hydrogel systems.

Motivated by the analytical results, specifically eqn (19), we next re-plot the experimental data using $\sqrt{t}/H$ as the x-axis coordinate, as shown in Fig. 5. The data can be compared to the analytical self-similar solution, rewritten in the form

$$\frac{\Delta(t)}{H} = \frac{2\Delta(\infty)}{H^2}\sqrt{\frac{Dt}{\pi}}, \tag{30}$$

for the initial stages of 1D swelling of the confined layers. By fitting a line to the initial slope of data for constrained swelling in Fig. 5,
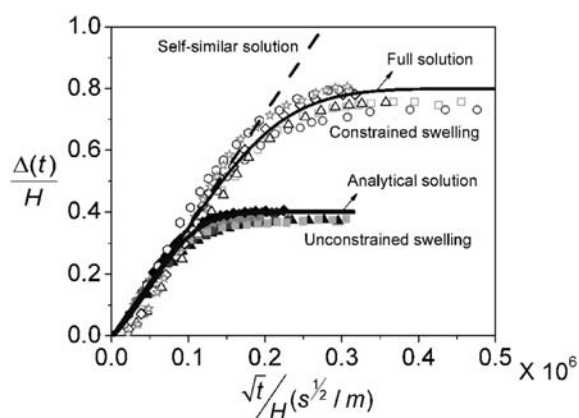
a value of $D = 1.5 \times 10^{-11}$ m^2 s^{-1} is obtained for the diffusivity. This value is consistent with literature reports of values for polyacrylamide[14,16] and PNIPAM[33,41,42] gels of similar composition, which are typically in the range of $D = 1$–3×10^{-11} m^2 s^{-1}.

The Poisson's ratio and diffusivity, along with the value of $\Delta(\infty)/H$ for one of the gels, completely prescribe the full analytical solution for constrained gels, eqn (23), and the numerical solution to eqn (29) for freely swelling gels. Thus, using the values of $\nu = 0.33$, $D = 1.5 \times 10^{-11}$ m^2 s^{-1} and $\Delta(\infty)/H = 0.80$, the average equilibrium degree of swelling for the constrained gels, we next plot the full solutions for each case in Fig. 5. As can be seen, the theoretical predictions match very well with the experimental data for both geometries; any systematic deviations are smaller in magnitude than the sample-to-sample variations and uncertainties in the measured values.

As described by eqn (15), swelling of the surface-attached gel generates an equibiaxial in-plane compressive stress proportional to the increase in layer thickness. This stress will induce a slight curvature in the underlying rigid substrate as described by the Stoney equation,[43] modified for the case of cylindrical bending where the film is much more compliant than the substrate, but not necessarily much thinner.[44] Once the constrained gel has reached its equilibrium degree of swelling, the force per unit length in the gel f is given by

$$f = \frac{E_s h_s^2}{6(1 - \nu_s^2)}\left(\frac{1}{R} - \frac{1}{R_0}\right)\left(1 + \frac{H + \Delta(\infty)}{h_s}\right)^{-1}, \tag{31}$$

where E_s and ν_s are the Young's modulus and Poisson's ratio of the substrate, respectively, h_s is the thickness of the substrate, R is the substrate radius of curvature, and R_0 the radius of curvature of the substrate in the absence of swelling stresses. Thus, by measuring the substrate radius of curvature it is possible to determine the value of f, and therefore the shear modulus using
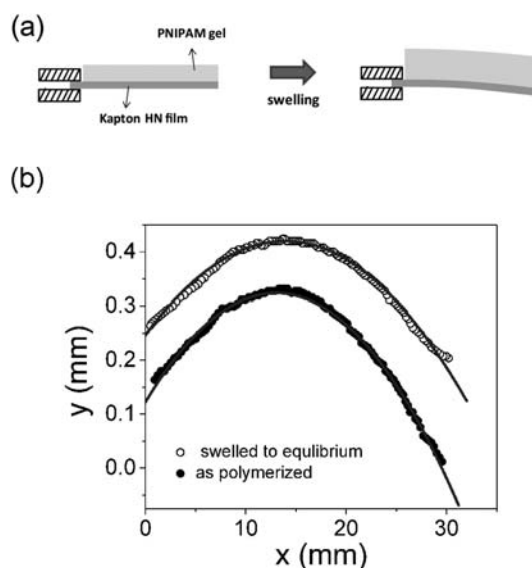

Fig. 5 A comparison between the theoretical predictions and experimental results for swelling kinetics of both constrained and unconstrained gels. A value of $D = 1.5 \times 10^{-11}$ m^2 s^{-1} was obtained from the initial slope of the constrained swelling curves, then used along with the equilibrium swelling ratios to plot the analytical solution, eqn (23), and the numerical solution to eqn (29) as solid lines. The self-similar solution of eqn (19), plotted as a dotted line, describes the early stage behavior of the constrained gel.

Fig. 6 (a) A schematic illustration of the substrate curvature measurement. (b) Measured x–y coordinates of the substrate (for a gel of thickness 504 µm on a Kapton substrate of 126 µm) along with best-fit curves to the equation of a circle; from the change in curvature, the shear modulus of the gel G was estimated as 220 Pa.

eqn (15). While the same principle has been used to fabricate sensors based on thin surface-attached gel layers,[45–47] we are not aware of any prior reports of using it to characterize gel mechanical properties.

To provide sufficient substrate curvature for straightforward measurement *via* optical microscopy, relatively thick gels ($H = 504$ μm) were coated on Kapton substrates ($E_s = 2.5$ GPa and $\nu_s = 0.34$) with $h_s = 76$ μm and 126 μm. As illustrated in Fig. 6a, the radius of curvature was determined by clamping the gel at one end and submerging it in a bath of water, positioned with the shorter in-plane dimension of the gel parallel to the optic axis of an optical microscope. From a series of micrographs taken along the length of the sample, the curvatures prior to swelling and after reaching equilibrium were determined by fitting the equation of a circle to the measured x–y coordinates of the substrate (Fig. 6b). For substrates of thickness of 76 and 126 μm, this yielded curvature changes of $(1/R - 1/R_0) = 1.5 \pm 0.2$ and 0.6 ± 0.1 m^{-1} at equilibrium swelling, respectively. Combined with a value of $\Delta(\infty)/H = 0.80$ from the data in Fig. 4, and eqn (15), we obtain respective values for the shear modulus of $G = 130 \pm 30$ Pa and 220 ± 40 Pa.

For comparison with these results, we also performed oscillatory shear rheology on a larger sample of gel of identical composition. Just after polymerization, the shear modulus was measured to be 1.3 ± 0.2 kPa from the value of G' in the plateau region of a strain-rate sweep, as shown in Fig. 7. After allowing the gel to swell to equilibrium in 3D, this value was reduced to 0.5 ± 0.1 kPa. While a direct comparison with literature values is difficult given the sensitivity of modulus to gel composition and polymerization conditions, the results from shear rheology fall in the same range as previously reported values of $G = 0.5$ kPa to 3.0 kPa for PNIPAM gels of similar composition.[48–50]

It is clear that our substrate curvature measurements underestimate the modulus compared to shear rheology. However, we note that discrepancies of this magnitude are not uncommon when comparing moduli of soft gels determined by different techniques.[24,51,52] Such measurements are often experimentally challenging to perform; even traditional shear rheology on soft gels is generally difficult and potentially subject to significant systematic errors. In addition, the linear poroelastic shear
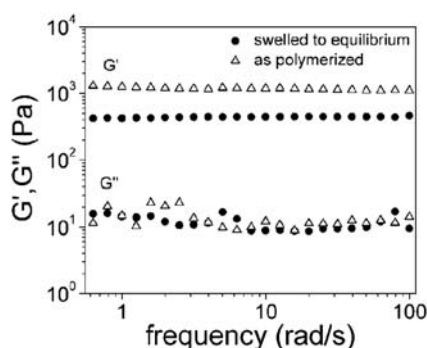
Fig. 7 Oscillatory shear rheology measurements (conducted at a stress of 1 Pa) on unconstrained gels following polymerization and after swelling to equilibrium. Values of the shear modulus were estimated from the storage modulus G' across this frequency range as 1.3 and 0.5 kPa, respectively.
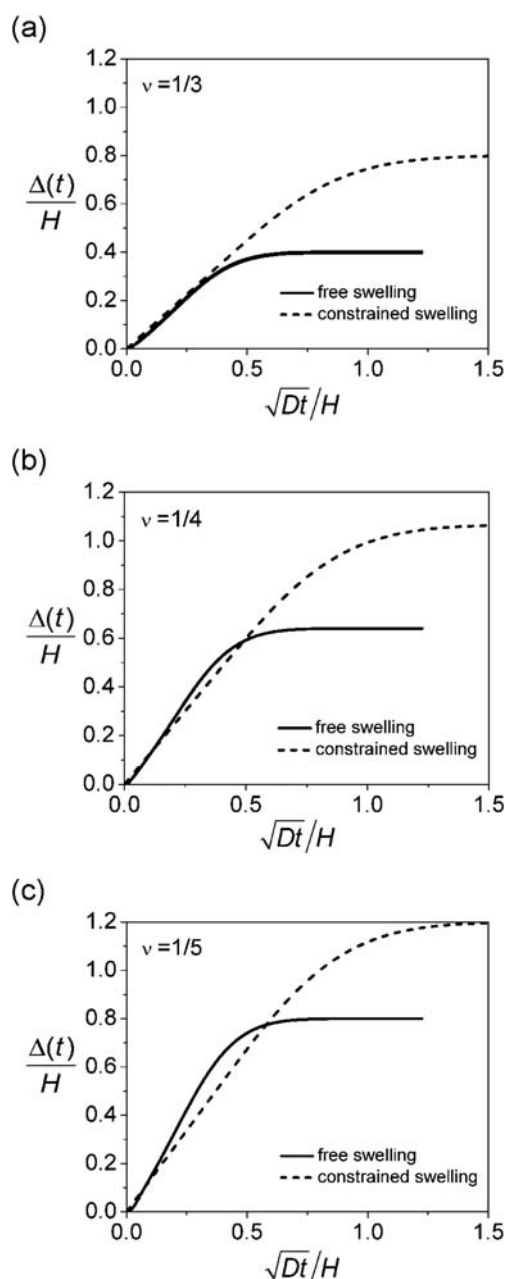
Fig. 8 Plots of the solutions to eqn (23) (free swelling) and (29) (constrained swelling) using the same values of gel modulus and solvent chemical potential as in Fig. 5, but with different values of Poisson's ratio ν. While the two curves nearly overlap at early times for the case of $\nu = 1/3$, this is not true in general, as seen clearly for the case of $\nu = 1/5$.

modulus does not capture changes in modulus due to swelling and is determined here at moderate strains, which may lead to sizable differences from the small-strain oscillatory shear modulus. Further work is required to determine whether closer correspondence between the values determined by substrate curvature and other techniques will be obtained using a non-linear model of gel behavior that explicitly accounts for these effects.

We next return to the definition of D (eqn (12)) to determine the third fundamental material parameter of the gel, the permeability k. Using the measured values of $D = 1.5 \times 10^{-11}$ m^2 s^{-1},
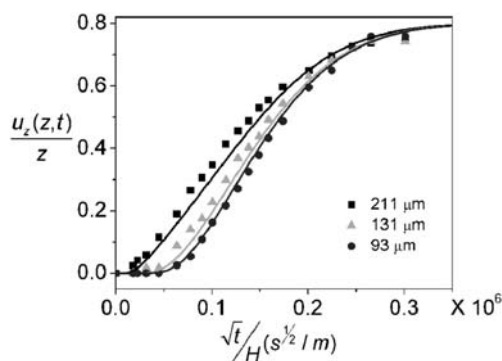
Fig. 9 A comparison between theory and experiment for vertical displacement of beads *within* a constrained gel layer. The initial gel thickness was 244 μm, and the values in the legend indicated the initial vertical distance from the substrate/gel interface. Good agreement between the data and predictions from eqn (22) reveals that linear poroelasticity also provides a reasonable description of the solvent distribution throughout the gel.

$G = 1.3$ kPa (the value for the unswelled gel from shear rheology), $\nu = 0.33$, and a value of $\eta = 1.0 \times 10^{-3}$ Pa s for water at 20 °C, we obtain an estimate of $k = 2.9 \times 10^{-18}$ m^2. If we compare this value to the permeability for laminar flow through a cylindrical tube of diameter d, *i.e.* $k = d^2/32$, we obtain a rough estimate for the average pore size of $d = 9.6$ nm. While measurements of pore size vary considerably depending on the technique employed and are complicated by the well known heterogeneity of gel structure, we note that a recent study employing several techniques yielded average pore diameters of 5–10 nm for polyacrylamide gels with similar monomer content to the PNIPAM gels studied here.[53]

Finally, we close with two further comments on our comparisons between experiment and linear poroelastic theory. First, the apparent collapse of the initial stage swelling data in Fig. 5 for *both swelling geometries* into a single curve raises the question of whether the self-similar solution, eqn (19), might be appropriate for treating the freestanding gel case as well as the surface-attached gel. However, the apparent equivalence between the two geometries is simply fortuitous, as shown in Fig. 8 where we plot the full solutions to eqn (23) and (29) using the same values of modulus and solvent chemical potential as in Fig. 5, but now with varying Poisson's ratio. For the case of $\nu = 1/3$ (Fig. 8a), similar to the experimental value, the two curves are nearly superimposed at early times. However, as ν is reduced to 1/4 or 1/5 (Fig. 8b and c, respectively), it is clear that the two curves are not the same, and that the 3D swelling geometry cannot in general be described by a straight line on this plot. We emphasize that this reflects the fact that there is *no self-similar solution* for the swelling of the freestanding layer. Since the strain in the directions of the film plane is equal to the average strain in the thickness direction, even in the initial stages of swelling the in-plane displacements cannot be neglected. Second, both the theory and our experimental method provide access to the time-dependent displacements at arbitrary spatial locations within the gel layer. In Fig. 9, we plot data for $u_z(z,t)/z$ for beads at several different positions z within a confined gel layer, along with the corresponding predictions from eqn (22). The agreement between theory and experiment is also quite good in this case, indicating that linear poroelastic theory not only provides

a suitable description of the *average* swelling of the film, but even captures the distribution of solvent through the layer thickness.

Conclusions

In conclusion, we have characterized the swelling kinetics of thin layers of poly(*N*-isopropylacrylamide) hydrogels under two simple geometries: free 3D swelling and constrained 1D swelling due to attachment to a rigid substrate. We find that Biot's theory of linear poroelasticity is adequate to describe both of these cases using only a single set of material parameters. This is a notable result, since although the incompleteness of Tanaka and co-workers' theory[14,15] has been pointed out by several authors,[19,21] few comparisons have been made between the predictions of poroelasticity and experimental data for swelling of polymer gels. The differential equations described by eqn (10) and (11) provide a straightforward starting point to model the swelling kinetics of gels and are amenable to numerical solution for more complicated geometries.

In addition to providing support for the validity of poroelastic theory to model swelling kinetics of polymer gels, the results of these experiments allow unambiguous determination of the three poroelastic material properties of the gel—the shear modulus, Poisson's ratio, and permeability—provided that the curvature of the substrate can be measured for the case of 1D swelling. This yields a very simple way to characterize the properties of thin gel layers that requires only an optical microscope and avoids the experimental complications and large sample sizes required for conventional shear rheology. While relatively thick samples (500 μm) were used here, by shifting to thinner substrates or a more sensitive curvature measurement, it should be possible to extend the technique to substantially thinner or lower modulus gels.

Acknowledgements

References

1 R. Duncan, *Nat. Rev. Drug Discovery*, 2003, **2**, 347.
2 N. A. Peppas, J. Z. Hilt, A. Khademhosseini and R. Langer, *Adv. Mater.*, 2006, **18**, 1345.
3 A. Richter, G. Paschew, S. Klatt, J. Lienig, K. Arndt and H. P. Adler, *Sensors*, 2008, **8**, 561.
4 P. Calvert, *Adv. Mater.*, 2009, **21**, 743.
5 K. Y. Lee and D. J. Mooney, *Chem. Rev.*, 2000, **101**, 1869.
6 S. Varghese and J. H. Elisseeff, *Adv. Polym. Sci.*, 2006, **203**, 95.
7 M. Kleverlaan, R. H. van Hoort and I. Jones, *Deployment of Swelling Elastomer Packers in Shell E&P*, SPE/IADC Drilling Conference held in Amsterdam, Netherlands, February, 2005.
8 S. Q. Cai, Y. C. Lou, P. Ganguly, A. Robisson and Z. G. Suo, *J. Appl. Phys.*, 2010, **107**, 103535.
9 K. Sekimoto, *J. Phys. II*, 1991, **1**, 19.
10 C. J. Durning and K. N. Morman, *J. Chem. Phys.*, 1993, **98**, 4275.
11 J. Dolbow, E. Fried and H. D. Jia, *J. Mech. Phys. Solids*, 2004, **52**, 51.

12 H. Li, R. Luo, E. Birgersson and K. Y. Lam, *J. Appl. Phys.*, 2007, **101**, 114905.
13 W. Hong, X. H. Zhao, J. X. Zhou and Z. G. Suo, *J. Mech. Phys. Solids*, 2008, **56**, 1779.
14 T. Tanaka, L. O. Hocker and G. B. Benedek, *J. Chem. Phys.*, 1973, **59**, 5151.
15 T. Tanaka and D. J. Fillmore, *J. Chem. Phys.*, 1979, **70**, 1214.
16 Y. Li and T. Tanaka, *J. Chem. Phys.*, 1990, **92**, 1365.
17 M. Doi and A. Onuki, *J. Phys. II*, 1992, **2**, 1631.
18 C. Y. Hui and V. Muralidharan, *J. Chem. Phys.*, 2005, **123**, 154905.
19 M. A. Biot, *J. Appl. Phys.*, 1941, **12**, 155.
20 M. Doi, *J. Phys. Soc. Jpn.*, 2009, **78**, 052001.
21 G. W. Scherer, *J. Non-Cryst. Solids*, 1989, **109**, 171.
22 C. Y. Hui, Y. Y. Lin, F. C. Chuang, K. R. Shull and W. C. Ling, *J. Polym. Sci., Part B: Polym. Phys.*, 2006, **43**, 359.
23 Y. Y. Lin and B.-W. Hu, *J. Non-Cryst. Solids*, 2006, **352**, 4034.
24 M. Galli, K. S. C. Comley, T. A. V. Shean and M. L. Oyen, *J. Mater. Res.*, 2009, **24**, 973.
25 Y. H. Hu, X. H. Zhao, J. J. Vlassak and Z. G. Suo, *Appl. Phys. Lett.*, 2010, **96**, 121904.
26 A. Peter and S. J. Candau, *Macromolecules*, 1986, **19**, 1952.
27 A. Peter and S. J. Candau, *Macromolecules*, 1988, **21**, 2178.
28 C. Wang, Y. Li and Z. Hu, *Macromolecules*, 1997, **30**, 4727.
29 T. Takigawa, K. Uchida, K. Takahashi and T. Masuda, *J. Chem. Phys.*, 1999, **111**, 2295.
30 A. Suzuki and T. Hara, *J. Chem. Phys.*, 2001, **114**, 5012.
31 T. Hajsz, I. Csetneki, G. Filipcsei and M. Zrinyi, *Phys. Chem. Chem. Phys.*, 2006, **8**, 977.
32 I. J. Suárez, A. Fernández-Nieves and M. Márquez, *J. Phys. Chem. B*, 2006, **110**, 25729.
33 J. Wahrmund, J.-W. Kim, L.-Y. Chu, C. Wang, Y. Li, A. Fernandez-Nieves, D. A. Weitz, A. Krokhin and Z. Hu, *Macromolecules*, 2009, **42**, 9357.
34 E. Alveroglu, A. Gelir and Y. Yilmaz, *Macromol. Symp.*, 2009, **281**, 174.
35 M. Speidel, A. Jonáš and E.-L. Florin, *Opt. Lett.*, 2003, **28**, 69.
36 M. M. Wu, J. W. Roberts and M. Buckley, *Exp. Fluids*, 2005, **38**, 461.
37 S. Hell, G. Reiner, C. Cremer and E. H. K. Stelzer, *J. Microsc. (Oxford, U. K.)*, 1993, **169**, 391.
38 Y. Li, Z. Hu and C. F. Li, *J. Appl. Polym. Sci.*, 1993, **50**, 1107.
39 S. Hirotsu, *J. Chem. Phys.*, 1991, **94**, 3949.
40 C. Li, Z. Hu and Y. Li, *Phys. Rev. E: Stat. Phys., Plasmas, Fluids, Relat. Interdiscip. Top.*, 1993, **48**, 603.
41 K. Takahashi, T. Takigawa and T. Masuda, *J. Chem. Phys.*, 2004, **120**, 2972.
42 K.-F. Arndt, M. Knörgen, S. Richter and T. Schmidt, NMR Imaging: Monitoring of Swelling of Environmental Sensitive Hydrogels, in *Modern Magnetic Resonance*, ed. Graham A. Webb, Springer, 2008, pp. 187–193.
43 G. G. Stoney, *Proc. R. Soc. London, Ser. A*, 1909, **82**, 172.
44 L. B. Freund and S. Suresh, *Thin Film Materials*, University Press, Cambridge, 2003.
45 R. Bashir, J. Z. Hilt, O. Elibol, A. M. Gupta and N. A. Peppas, *Appl. Phys. Lett.*, 2002, **81**, 3091.
46 Y. Zhang, H. F. Ji, D. Snow, R. Sterling and G. M. Brown, *Instrum. Sci. Technol.*, 2004, **32**, 361.
47 J. Z. Hilt, A. M. Gupta, R. Bashir and N. A. Peppas, *Biomed. Microdevices*, 2003, **5**, 177.
48 X. Xia, J. Yih, N. A. D'Souza and Z. Hu, *Polymer*, 2003, **44**, 3389.
49 J. Nie, B. Du and W. Oppermann, *Macromolecules*, 2004, **37**, 6558.
50 M. Guenther, G. Gerlach, D. Kuckling, K. Kretschmer, C. Corten, J. Weber, J. Sorber, G. Suchaneck and K.-F. Arndt, *Proc. SPIE*, 2006, **6167**, 61670T1.
51 G. Constantinides, Z. I. Kalcioglu, M. McFarland, J. F. Smith and K. J. Van Vliet, *J. Biomech.*, 2008, **41**, 3285.
52 S. Kundu and A. J. Crosby, *Soft Matter*, 2009, **5**, 3963.
53 J. Wang, A. D. Gonzalez and V. M. Ugaz, *Adv. Mater.*, 2008, **20**, 4482.